CZU: 548.736.3 + 547.587.11 https://doi.org/10.59295/mabt2026.17

4-AMINOSALICYLIC ACID – 4-ACETYLPYRIDINE COCRYSTAL: SYNTHESIS, CRYSTAL STRUCTURE AND HIRSHFELD SURFACE ANALYSIS

Anastasia GOROBET, Marina S. FONARI, Lilia CROITOR

Institute of Applied Physics, Moldova State University, Academy str, 5 MD2028, Chisinau, Moldova

Abstract

A new cocrystal of pharmaceutically relevant 4-aminosalicylic acid (ASA) with 4−acetylpyridine (AP) was obtained by solvent co-crystallization from methanol and characterized. The ASA−AP binary product crystallizes in the monoclinic space group P21/n, with a = 7.032(2), b = 15.2527(19), c = 12.7106(14) Å; β = 105.48(2), V = 1313.8(4) Å3, Z = 4. The ASA and AP molecules are present in a 1:1 molar ratio in the asymmetric unit. Classical O−H···N and non-classical C−H···O hydrogen bonds stabilize the supramolecular architecture through the interplay of homomeric and heteromeric supramolecular motifs. The acid–pyridine O–H···N hydrogen bond plays a key role in the formation of the supramolecular assembly. In addition, Hirshfeld surface analysis provides deeper insight into the distribution of intermolecular interactions in the cocrystal.

Keywords: cocrystal, 4-aminosalicylic acid, 4-acetylpyridine, hydrogen bonding, crystal structure, Hirshfeld surface analysis.

Introduction

Cocrystals are homogeneous crystalline materials composed of two or more distinct neutral molecules in a definite stoichiometric ratio, connected through non-covalent interactions such as hydrogen bonds [1, 2]. One of the main advantages of cocrystals is their ability to modify physicochemical properties without covalent modification of the constituent molecules, allowing regulation of solubility, dissolution rate, stability, and other material characteristics [1, 2]. 4-Aminosalicylic acid (ASA, also known as para-aminosalicylic acid) is an antibiotic primarily used to treat tuberculosis (TB) by inhibiting folic acid synthesis, and a local anti-inflammatory agent for inflammatory bowel disease (IBD). It is also used in combination with other antituberculosis medications (e.g., isoniazid) to treat multi-drug-resistant TB [3]. The inspection of literature sources revealed the thought-provoking examples of ASA cocrystals obtained by different cocrystallization techniques. André et al. reported the multicomponent ASA solids as solvates and molecular salts with dioxane, morpholine and piperazine obtained by grinding/kneading and solution methods [4]. Polymorphic modifications were observed for the ASA cocrystals with sulfadimidine (SD) prepared via liquid-assisted milling or the spray drying [5]. The variation in stoichiometry was reported for the ASA cocrystals with the anticonvulsant drug carbamazepine (CBZ) that led to dramatic decrease of the CBZ rate of conversion from anhydrous to the hydrated form, and as a consequence, to approximately 1.5 times solubility improvement [6]. To optimize the low solubility of ASA that strictly limits its absorption and clinical application, Tang et al. reported the ASA-nicotinamide (NCT) cocrystal obtained by the grinding method that demonstrated the solubility increase by more than 20 times for the cocrystal [7]. The influence of solution composition and solvent on the cocrystallization outcome, and the applicability of the ΔpKa rule was shown on a set of ASA multicomponent solids with various pyridine-based compounds [8]. The literature sources reveal no principal restrictions in using liquid or low melting compounds as coformers [9-14]. Pyridine derivatives are frequently used as coformers due to the strong hydrogen-bond-acceptor ability of the pyridine nitrogen. 4-Acetylpyridine (AP), a liquid under ambient conditions, is suitable as a coformer. Additionally, AP exhibits a wide range of biological activities, including antiproliferative effects against human cancer cell lines in trans-[$PtCl_2$(4-acetylpyridine)$_2$] complexes [15].

In this paper, we applied a cocrystal strategy to combine 4-aminosalicylic acid (ASA) with 4-acetylpyridine (AP), to obtain the corresponding cocrystal, ASA-AP.

Results and Discussion

Synthesis and Crystallization. The starting reagents, 4-aminosalicylic acid (ASA) and 4-acetylpyridine (AP) were obtained from commercial suppliers and used without further purification. A mixture of 4-acetylpyridine (0.011 mL, 0.1 mmol) and 4-aminosalicylic acid (15.3 mg, 0.1 mmol) was dissolved in 10 mL of methanol. The reaction mixture was refluxed at 60 °C for 4 h to give a clear solution. After filtration, the solution was left to evaporate slowly at room temperature, yielding crystals ASA-AP suitable for single crystal X-ray diffraction.

X-ray study. The single crystal X-ray data were collected at room temperature on an Xcalibur E diffractometer equipped with a CCD area detector and a graphite monochromator utilizing MoK_{α} radiation at room temperature. Structure solution, refinement, and data output were carried out with the SHELXTL program [16]. The crystal structure was refined as a two-component twin. Non-hydrogen atoms were refined in anisotropic approximation. The hydrogen atoms were placed in geometrically calculated positions with reference to C–O distances and C–N–C angles that corresponded to the neutrality of the cocrystal components. The X–ray data and the details of the refinement for ASA-AP are summarized in Table 1. Complete information about the crystal structure and molecular geometry is available in CIF file deposited in the Cambridge Crystallographic Data Centre, CCDC deposition number 2539113. These data can be obtained free of charge via https://www.ccdc.cam.ac.uk/deposit, or e-mail: deposit@ccdc.cam.ac.uk.

Table 1. Crystal data and structure refinement details for ASA-AP cocrystal.

Compound	ASA-AP
Empirical formula	$C_{14}H_{14}N_2O_4$
Formula weight	274.27
Temperature, K	295(2)
Crystal system	Monoclinic
Space group	$P2_1/n$
Unit cell dimensions	
a, Å	7.032(2)
b, Å	15.2527(19)
c, Å	12.7106(14)
b, °	105.48(2)
*V*olume, Å^3	1313.8(4)
Z	4
D(calcd), g/cm^3	1.387
μ, mm^{-1}	0.103
F(000)	576
Reflections collected	8466
Independent reflections	2381 [*R*(int) = 0.0762]
Data / restraints / parameters	2381 / 3 / 191
Goodness-of-fit on F^2	0.951
Final *R* indices [$I>2\sigma(I)$] R_1, wR_2	0.0800, 0.1944
R indices (all data), R_1, wR_2	0.1595, 0.2440

The cocrystal ASA−AP crystallizes in the centrosymmetric monoclinic space group $P2_1/n$. The ASA and AP molecules are present in a 1:1 molar ratio and occupy general positions in the unit cell. Both molecules have planar skeletons. The twisted angle between the phenyl ring and

the carboxylic group in ASA is 1.97(4)°, while the twisted angle between the acetyl group and the pyridine ring in AP is 2.88(5)°. The planar conformation of ASA is stabilized by the intramolecular OH···O hydrogen bond, O(3)–H(3A)···O(1) (H···O, O···O 1.87, 2.579(4) Å) in the form of $S_1^1(6)$ H-bonded graph set (Fig. 1a, Table 2). The neutrality of both components in cocrystal is justified by the molecular geometries, namely, by non-equalised C–O bond distances, C(1)–O(1) 1.227(5) and C(1)–O(2) 1.324(5) Å, with the H atom localized near the carboxylic group and the elongated C–O(H) bond compared with the C=O bond of the carbonyl group. The molecules form linear binary adduct via robust acid-base $R_2^2(7)$ supramolecular synthon originated from association of one OH···N and one CH···O hydrogen bond (Table 2), which is the main structure-directing force typical for the acid-pyridine-base cocrystals [8]. This $R_2^2(7)$ H-bonded pattern is roughly planar, arranging ASA and AP molecules nearly in the same plane, as indicated by an ASA/AP interplanar angle of 1.94(2)°. The ASA molecules, related by the two-fold screw axis, also exhibit a self-association homomeric H-bonded motif. They form the H-bonded chain *via* N(1)-H…O(2) hydrogen bond, while the second amino H-atom participates in an acid-base N(1)-H…O(4) H-bond involving the carbonyl oxygen atom of the AP coformer, resulting in a stair-case double tape motif with chains lying in planes separated by 1.665 Å (Fig. 1b). These H-bonded tapes pack in a stacking arrangement, forming columns with alternating ASA and AP molecules. The π-π stacking is efficient, with $Cg_1 \ldots Cg_2$ separations alternating as 3.840(4) and 3.850(4) Å (Fig. 1 c, d).

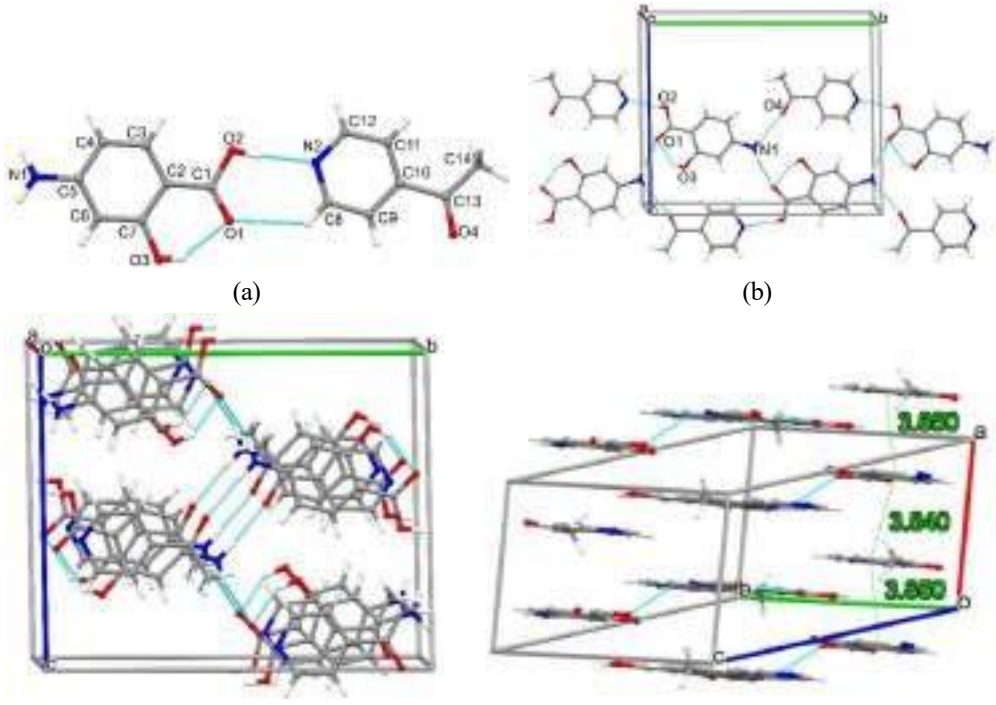
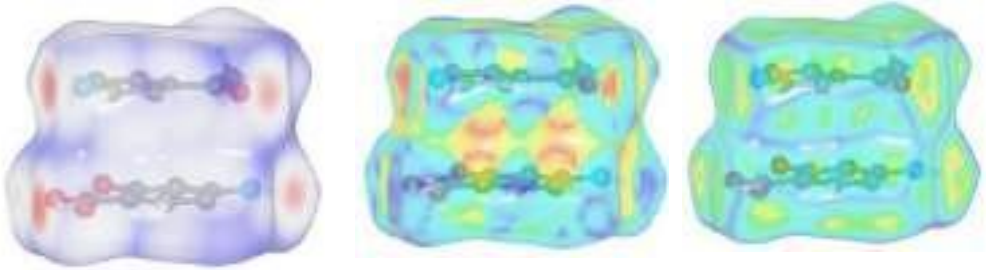


Figure 1. Crystal structure of ASA-AP cocrystal. (a) View of formula unit; (b) H-bonded tape running along the b-axis; (c) view of stacking columns along the a-axis; (d) crystal packing with indication of Cg1…Cg2 distances.

Table 2. Hydrogen bonds for ASA-AP cocrystal [Å and °].

Donor-H···Acceptor	d(D-H)	d(H···A)	d(D···A)	∠(DHA)	Symmetry transformations for acceptor
N(1)–H(1N)···O(1)	0.86(2)	2.51(4)	3.232(6)	143(6)	1/2-*x*, *y*+1/2, 3/2-*z*
N(1)–H(2N)···O(4)	0.86(2)	2.11(2)	2.963(6)	174(6)	1-*x*, 1-*y*, 1-*z*
O(2)–H(2)···N(2)	0.82	1.86	2.682(4)	175.7	1-*x*, -*y*, 1-*z*
O(3)–H(3A)···O(1)	0.82	1.87	2.579(4)	144.1	*x*, *y*, *z*
C(8)–H(8)···O(1)	0.93	2.47	3.176(6)	132.4	1-*x*, -*y*, 1-*z*

Hirshfeld surface analysis of the ASA-AP cocrystal. The Hirshfeld surface (HS) [17] analysis and the two-dimensional (2D) fingerprint plots [18], generated using the CrystalExplorer21 [19] program which have been successfully applied for analysis of cocrystals [12, 13], were applied to investigate both the qualitative and quantitative contributions of intermolecular interactions in the crystal structure of the ASA-AP cocrystal. In order to evaluate the effect of cocrystal formation on intermolecular interactions, the obtained contact contributions were additionally compared with those calculated for the individual components, 4-aminosalicylic acid (ASA) and 4-acetylpyridine (AP). The HS mapped over the normalized contact distance (d_{norm}), shows several pronounced red spots corresponding to short intermolecular contacts (Fig. 2a). These regions mainly indicate strong hydrogen bonds of the O–H···N and N–H···O types formed between the functional groups of the two molecular components of the cocrystal, which play a key role in stabilizing the crystal structure. The representation of the HS using the shape index function reveals alternating red and blue triangular regions characteristic of aromatic stacking interactions (Fig. 2b). These patterns suggest the presence of weak π···π interactions between the aromatic rings of the molecules, which additionally contribute to the supramolecular organization of the crystal. Curvedness (Fig. 2c), specified as the "sharpness" of a surface, clearly indicates the relatively large flat regions (green) for both contributing molecules separated by dark blue edges. The extended flat areas in ASA and AP are in line with the X-ray observations for the favorable planar stacking arrangement of molecules in the ASA-AP cocrystal.



(a) (b) (c)

Figure 2. Hirshfeld surface mapped with (a) dnorm, (b) shape index, and (c) curvedness for ASA-AP.

The decomposition of the 2D fingerprint plots reveals main types of intermolecular contacts in ASA-AP cocrystal (Fig. 3).

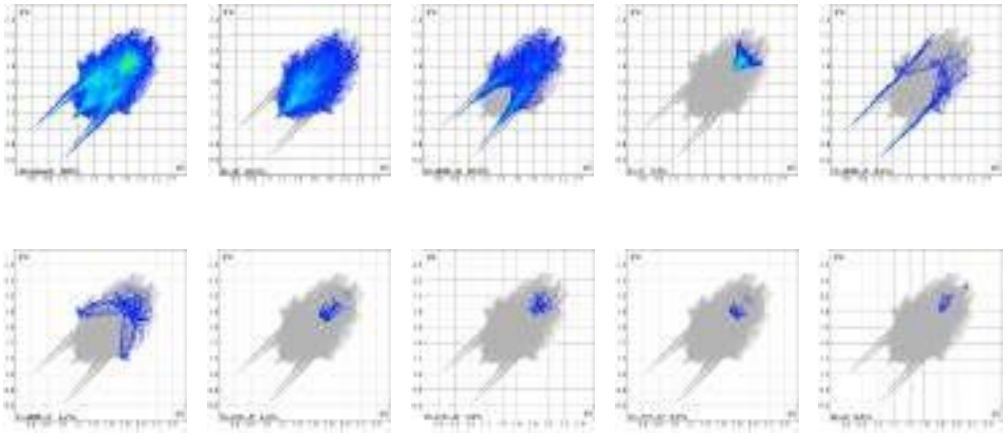


Figure 3. Overall 2D plots of intermolecular contacts distribution in ASA-AP cocrystal.

The largest contribution to the total HS area arises from H···H contacts, which account for approximately 48.9% of the total interactions in the cocrystal, compared with 39.5% in pure ASA and 45.4% in AP, reflecting the predominance of van der Waals interactions in the crystal packing. The O···H/H···O contacts, mainly associated with hydrogen bonds involving the hydroxyl, carbonyl, and amino groups of the ASA molecule, contribute about 29.9% to the total surface in the cocrystal, in comparison with 34.0% in ASA and 17.4% in AP. The slightly lower contribution relative to pure ASA suggests that some homomeric ASA hydrogen bonds are replaced by heteromeric interactions between ASA and AP molecules in the cocrystal. The N···H/H···N contacts account for approximately 6.4% of the Hirshfeld surface in the ASA-AP cocrystal, whereas they represent 0.7% in ASA and 14.0% in AP. This contribution reflects the formation of heteromeric hydrogen bonds involving the pyridine nitrogen atom of AP and the hydrogen-bond donor groups of ASA, including the characteristic O–H···N acid–pyridine interaction responsible for the formation of the R_2^2 (7) supramolecular heterosynthon observed in the crystal structure. A smaller contribution is observed for C···C contacts, which represent approximately 7.3% of the total HS in the cocrystal, compared with 12.4% in ASA and 8.2% in AP, indicating π···π interactions between cyclic moieties. These interactions are consistent with the stacking columns of alternating ASA and AP molecules observed in the crystal packing. Additionally, H···C/C···H contacts contribute approximately 4.4% to the total surface in the cocrystal, compared with 6.6% in ASA and 10.0% in AP, and may be associated with weak C–H···π interactions. Minor contributions arise from other intermolecular contacts such as N···O/O···N (0.6% in the cocrystal; 0% in ASA; 0.6% in AP), O···O (0.3% in the cocrystal; 0.5% in ASA; 0% in AP), and O···C/C···O interactions (1.0% in the cocrystal; 3.4% in ASA; 3.2% in AP) (Fig. 4)

Overall, the comparative Hirshfeld surface analysis indicates that the crystal packing of the ASA-AP cocrystal is dominated by H···H and O···H/H···O interactions, while the presence of significant N···H/H···N contacts reflects the formation of heteromolecular hydrogen bonds between the acid and pyridine functional groups. These interactions play a decisive role in directing the supramolecular assembly, whereas π···π stacking and weaker contacts provide additional stabilization of the crystal structure.

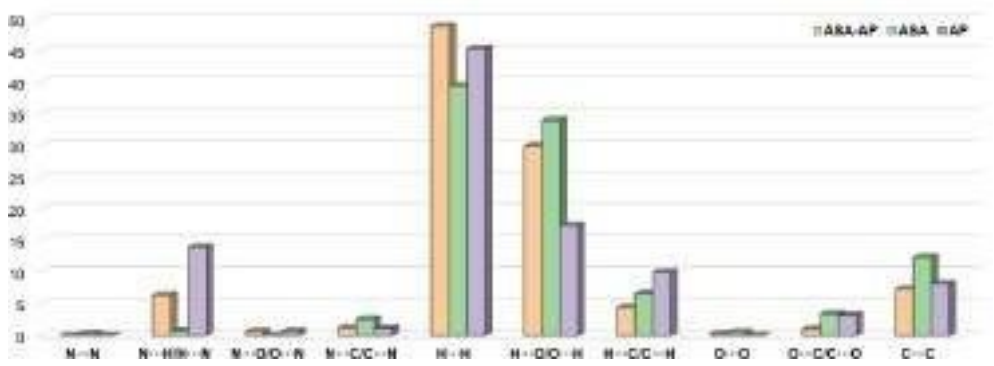


Figure 4. Distribution of intermolecular contacts in ASA-AP cocrystal in comparison with ASA and AP pure forms.

In conclusion, new cocrystal, ASA-AP, was obtained by cocrystallization from methanol. The robust acid···pyridine supramolecular heterosynthon occurs even in the presence of other competing H-bonding functional groups. The H-bonds in the crystal generate infinite supramolecular tapes, with the components arranged in nearly planar fashion, while π-π stacking interactions between these arrays stabilise the parallel stacking patterns. Hirshfeld surface analysis further confirmed the importance of these intermolecular interactions, showing that H···H, O···H/H···O, and N···H/H···N contacts dominate the crystal packing, while π···π and weaker interactions provide additional stabilization of the structure.

Acknowledgement

The authors thank the Subprogram 011202 financed by the Ministry of Education and Research of R. Moldova.

References

1. Physicohemical Properties. Crystal Growth and Design, 2009, 9, 2950-2967, https://doi.org/10.1021/cg900129f
2. DUGGIRALA, N. K., PERRY, M. L., ALMARSSON, Ö., ZAWOROTKO, M. J., Pharmaceutical Cocrystals: Along the Path to Improved Medicines. Chem. Commun., 2016, 52, 640-655, https://doi.org/10.1039/C5CC08216A.
3. DONALD, P. R., DIACON, A. H. Para-aminosalicylic acid: the return of an old friend. The Lancet. Infectious Diseases, 2015, 15, 1091–1099, doi:10.1016/s1473-3099(15)00263-7.
4. ANDRÉ, V., BRAGA, D., GREPIONI, F., DUARTE, M. T. Crystal Forms of the Antibiotic 4-Aminosalicylic Acid: Solvates and Molecular Salts with Dioxane, Morpholine, and Piperazine, Cryst. Growth Des. 2009, 9, 5108–5116, https://doi.org/10.1021/cg900495s.
5. GROSSJOHANN, C.; SERRANO, D. R.; PALUCH, KRZYSZTOF J.; O'CONNELL, P.; VELLA-ZARB, L.; MANESIOTIS, P.; MCCABE, T.; TAJBER, L.; CORRIGAN, O. I.; HEALY, A. M. Polymorphism in sulfadimidine/4- aminosalicylic acid cocrystals: solid-state characterization and physicochemical properties. Journal of Pharmaceutical Sciences, 2015, 104, 1385-1398, https://doi.org/10.1002/jps.24345
6. DROZD, K. V., MANIN, A. N., PERLOVICH, G. L., Novel drug–drug cocrystals of carbamazepine with para-aminosalicylic acid: screening, crystal structures and comparative study of carbamazepine cocrystal formation thermodynamics. CrystEngComm, 2017, 19, 4273-4286, https://doi.org/10.1039/C7CE00831G
7. TANG, Y., ZHANG, L., HUANG, Y., YANG, D. Characterizing the structure of a p-aminosalicylic acid and nicotinamide drug cocrystal via terahertz spectroscopy. CrystEngComm, 2026, 28, 1091-1104, https://doi.org/10.1039/D5CE01165E

8. GOSWAMI, P. K., THAIMATTAM, R., RAMANAN, A. Crystal engineering of multicomponent crystal forms of p-aminosalicylic acid with pyridine based coformers, Cryst. Growth Des. 2016, 16, 1268–1281, https://pubs.acs.org/doi/10.1021/acs.cgd.5b01308
9. DRAGUTA, S., YAKOVENKO, A. A., FONARI, M. S., TIMOFEEVA, T. V. Unusual Chemical Ratio, Z′ Values, and Polymorphism in Three New N-Methyl Aminopyridine−4-Nitrophenol Adducts. Cryst. Growth Des., 2014, 14, 3423−3433, https://doi.org/10.1021/cg500360f
10. EJARQUE, D., CALVET, T., BARDIA, M. F., PONS, J. Virtual assessment achieved two binary cocrystals based on a liquid and a solid pyridine derivative with modulated thermal stabilities, CrystEngComm, 2023, 25, 4798-4811, https://doi.org/10.1039/D3CE00608E
11. DAISY RANI, T., RAJKUMAR, M., CHANDRAMOHAN, A. Synthesis, crystal structure, thermal, mechanical and laser damage threshold studies of an NLO active organic molecular adduct: 4-Acetylpyridine:4-aminobenzoic acid. Mater. Lett. 2018, 222, 118-121, https://doi.org/10.1016/j.matlet.2018.03.195
12. THOMAS, L. H., CRAIG, G. A., GUTMANN, M. J., PARKIN, A., SHANKLAND, K., WILSON, C. C. Conformational polymorphism of the molecular complex of 3-fluorobenzoic acid with 4-acetylpyridine. CrystEngComm, 2011, 13, 3349-3354, https://doi.org/10.1039/C1CE05139C
13. SRIJANA, P. J., KARTHICK, T., NARAYANA, B., SAROJINI, B. K., WONG, Q. A., QUAH, C. K. LIKHITHA U. 4 - Acetylpyridine - succinic acid cocrystal: Synthesis, X-ray structure, DFT and Hirshfeld surfaces analysis, Molecular Crystals and Liquid Crystals, 2024, 768, 47-62, https://doi.org/10.1080/15421406.2023.2300908
14. SINGH, M., ANTHAL, S., SRIJANA, P. J., NARAYANA, B., SAROJINI, B. K., LIKHITHA, U., KAMAL, R. K. Novel supramolecular co-crystal of 3-aminobenzoic acid with 4-acetyl-pyridine: Synthesis, X-ray structure, DFT and Hirshfeld surface analysis. Journal of Molecular Structure, 2022, 1262, 133061 https://doi.org/10.1016/j.molstruc.2022.133061
15. RAKIĆ, G. M., GRGURIĆ-ŠIPKA, S., KALUCEROVIC, G. N., GÓMEZ-RUIZ, S., BJELOGRLIĆ, S. K., RADULOVIĆ, S. S., TEŠIĆ, Ž. LJ. Novel trans-dichloridoplatinum(II) complexes with 3- and 4-acetylpyridine: Synthesis, characterization, DFT calculations and cytotoxicity. European Journal of Medicinal Chemistry, 2009, 44, 1921-1925, https://doi.org/10.1016/j.ejmech.2008.11.004
16. SHELDRICK, G. M. A short history of SHELX. Acta Crystallographica, 2008, A64, 112–122, https://doi.org/10.1107/S0108767307043930.
17. HIRSHFELD, F. L. Bonded-Atom Fragments for Describing Molecular Charge Densities. Theoretica Chimica Acta, 1977, 44, 129-138. https://doi.org/10.1007/BF00549096
18. SPACKMAN, M. A. AND JAYATILAKA, D. Hirshfeld Surface Analysis. CrystEngComm, 2009, 11, 19-32. https://doi.org/10.1039/B818330A
19. WOLFF, S. K., GRIMWOOD, D. J., MCKINNON, J. J., TURNER, M. J., JAYATILAKA, D., SPACKMAN, M. A. CrystalExplorer, University of Western Australia, Australia. 2012.

Authors:



Anastasia GOROBET, Scientific Researcher,
Institute of Applied Physics, Moldova State University, Chisinau, Moldova
E-mail: nasteagorobet@gmail.com
ORCID: 0000-0002-6850-1456



Marina S. FONARI, PhD in chemistry, leading scientific worker, Institute of Applied Physics, Moldova State University, Chisinau, Moldova
E-mail: fonari.xray@gmail.com
ORCID: 0000-0002-2508-5368



Lilia CROITOR, PhD in chemistry, leading scientific worker, Institute of Applied Physics, Moldova State University, Chisinau, Moldova
E-mail: croitor.lilia@gmail.com
ORCID: 0000-0003-0757-7358